This is an open access article published under an ACS AuthorChoice License, which permits copying and redistribution of the article or any adaptations for non-commercial purposes.

analytical chemistry

Letter

pubs.acs.org/ac

UV–Visible and Plasmonic Nanospectroscopy of the CO_2 Adsorption Energetics in a Microporous Polymer

Ferry A. A. Nugroho,[†] Chao Xu,[‡] Niklas Hedin,[‡] and Christoph Langhammer*[,†]

[†]Department of Applied Physics, Chalmers University of Technology, SE-412 96, Göteborg, Sweden

[‡]Department of Materials and Environmental Chemistry, Berzelii Center EXSELENT on Porous Materials, Arrhenius Laboratory, Stockholm University, SE-106 91, Stockholm, Sweden

Supporting Information

ABSTRACT: In the context of carbon capture and storage (CCS), micro- and mesoporous polymers have received significant attention due to their ability to selectively adsorb and separate CO_2 from gas streams. The performance of such materials is critically dependent on the isosteric heat of adsorption (Q_{st}) of CO_2 directly related to the interaction strength between CO_2 and the adsorbent. Here, we show using the microporous polymer PIM-1 as a model system that its Q_{st} can be conveniently determined by *in situ* UV–vis optical transmission spectroscopy directly applied on the adsorbent or, with higher resolution, by indirect nanoplasmonic sensing based on localized surface plasmon resonance in metal nanoparticles. Taken all together, this study provides a general blueprint for efficient *optical* screening of micro- and mesoporous polymeric materials for CCS in terms of their CO_2 adsorption energetics and kinetics.

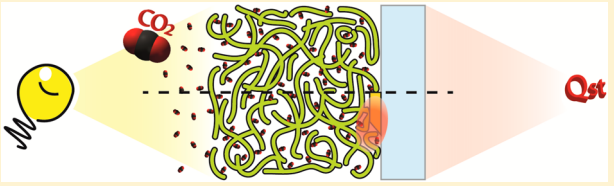

Atmospheric CO_2 is in the spotlight in the wake of constantly increasing global temperature, where it is pinned as the single most important factor in the anthropogenic greenhouse effect.[1] Therefore, numerous mitigation strategies for CO_2 emission reductions are suggested or already actively being applied. One particular direction is the CCS scheme, which has accelerated the search for materials that can capture CO_2 at a lower cost than today's. In this context, micro- and mesoporous materials such as polymers, zeolites, or metal–organic frameworks (MOFs) have received particular attention.[2−7] Capture of CO_2 with these materials exploits that CO_2 *selectively* adsorbs from gas mixtures and can be recovered as nearly pure CO_2 by cyclically increasing the temperature or decreasing the pressure. For a successful CO_2 capture, the CO_2-adsorbent interaction strength should be engineered in an optimal way.[5] This interaction is typically assessed by measuring the isosteric heat of adsorption (Q_{st}) using gravimetric, volumetric, calorimetric, or to some extent chromatographic (carrier gas) techniques. The latter are simple and inexpensive but not very accurate. Gravimetric techniques are complicated by buoyancy and Knudsen diffusion at low pressure, volumetric techniques need accurate dead space determinations for volume correction, and calorimetric techniques are expensive and complex.[8] Furthermore, porous polymer systems (as well as, e.g., MOFs) potentially show swelling upon CO_2 adsorption, which further complicates traditional analysis.[9]

As an attractive alternative, we show here that accurate direct measurements of the Q_{st} of CO_2 for microporous polymers become conveniently available by (i) simple *in situ* UV–vis optical spectroscopy directly applied on the adsorbent or (ii) by indirect nanoplasmonic sensing (INPS)[10] based on localized surface plasmon resonance (LSPR) in metal nanoparticles.[11] As we show, INPS has a higher resolution than traditional spectroscopy owing to the superior sensitivity of plasmonic sensors.[12−14] We use gold plasmonic sensor nanodisks with dimensions in the 100 nm size range on a transparent support. The nanodisks and the support (Figure 1) are coated with a 10 nm thick dielectric spacer layer to tailor the surface chemistry (here we used Si_3N_4). The INPS sensors monitor the surface specific changes occurring on the spacer layer or in its close vicinity via the strongly enhanced plasmonic electromagnetic field, which extends a few tens of nanometers beyond the spacer layer surface.[10] Since the adsorbed CO_2 molecules slightly change the refractive index of the adsorbent within the enhanced field region, a spectral shift of the plasmon extinction peak (λ_{peak}) is induced, which is used as the readout with a reported resolution limit of 0.01 nm.[15]

To demonstrate and benchmark our approach, we use a well-established polymer with intrinsic microporosity, PIM-1,[16,17] as a CO_2 adsorbent model system. This class of polymers is attractive for CCS and other gas separation processes as they are easy to prepare and process, and have high gas permeability and selectivity.[18−20] In addition, PIM-1 exhibits a light absorption band below ~480 nm, which makes direct UV–vis spectroscopy with reasonable optical contrast possible. A schematic depiction of our approach and sample design is shown in Figure 1. The PIM-1 is deposited as a thin film on an INPS sensor chip by spin coating.

Received: August 13, 2015
Accepted: September 28, 2015
Published: September 28, 2015

 © 2015 American Chemical Society

DOI: 10.1021/acs.analchem.5b03108
Anal. Chem. 2015, 87, 10161−10165

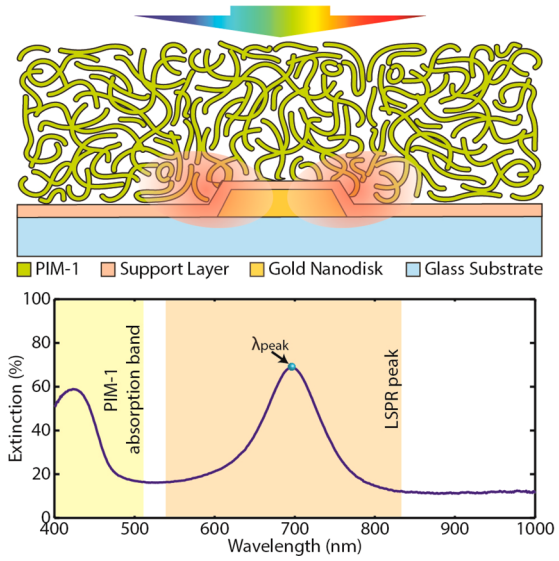

Figure 1. (Top) Sample configuration with a thin film of a polymer with intrinsic microporosity (PIM-1) spin coated onto an indirect nanoplasmonic sensor (INPS) chip, comprised of a glass substrate decorated with a quasi-random array of plasmonic gold nanodisks (not drawn to scale). Under white light illumination, the locally enhanced electric field created via excitation of localized surface plasmon resonance (LSPR) in the gold nanodisks gives rise to a sensing volume that extends a few tens of nanometers from the gold nanodisk surface. Within it, CO_2 adsorption in the PIM-1 can be detected via a corresponding local change in optical permittivity, which slightly alters the resonance condition of the plasmon excitation in the Au nanodisks. (Bottom) A corresponding optical extinction spectrum of a INPS chip with a 610 nm thick PIM-1 film. Its two distinct bands originate from the PIM-1 itself (400−500 nm) and from the LSPR in the Au nanodisks (600−800 nm).

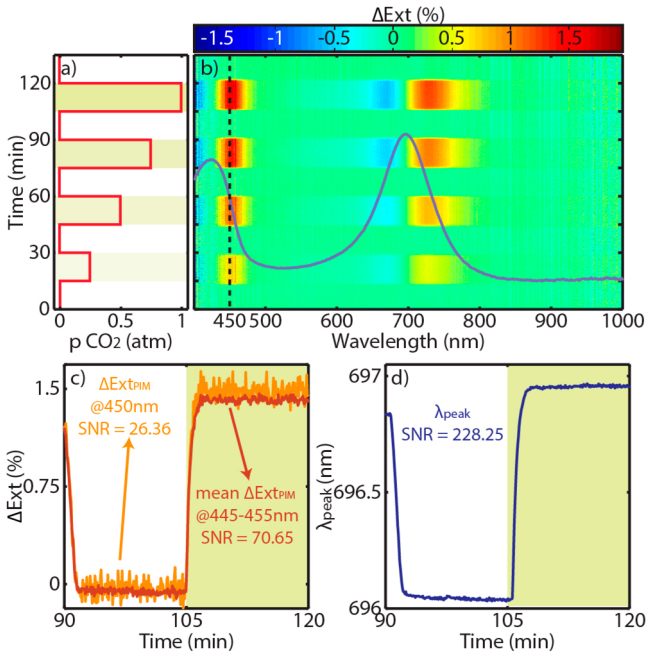

Figure 2. (a) Typical cycle of different CO_2 partial pressure for measuring the CO_2 adsorption isotherm. (b) Corresponding color coded optical extinction change ΔExt (with respect to $t = 0$) measured at 298 K. The inserted optical spectrum is obtained at 298 K in pure Ar carrier gas. The ΔExt readout changes on both sides of the LSPR peak and the absorption band maximum of the PIM-1, as responses to the CO_2 pressure. The ΔExt for the PIM-1 absorption band, ΔExt_{PIM}, is the largest at 450 nm (dashed line). (c) Direct UV−vis spectroscopy readout for the apparent (i.e., convoluted by instrument response time) CO_2 adsorption and desorption kinetics after a 1 atm CO_2 pulse, tracked at 450 nm (orange line) or by the mean ΔExt_{PIM} in the range of 445−455 nm (red line). Note the improvement of the SNR. (d) INPS response from the same sample for a 1 atm CO_2 pulse. Note the significantly better SNR compared to the direct UV−vis signal.

A typical extinction spectrum for the INPS chip with the thin PIM-1 film is also shown in Figure 1. It has two distinct bands: one in the near UV region from the PIM-1, and a second one, labeled by λ_{peak}, at ∼700 nm, from the LSPR of the Au nanodisks. To separate these two peaks, we *tune* the spectral position of the LSPR peak by tailoring the dimensions of the nanodisks. This spectral separation allows us to address both bands simultaneously but independently as plasmonic (by sensing of dielectric changes upon CO_2 sorption via the enhanced near fields of the plasmonic particles)[13,14,21] or direct UV−vis readouts, respectively.

An example of wavelength-resolved optical response to variation in the CO_2 pressure is shown in Figure 2. Distinct increase (right) or decrease (left) of the ΔExt signal occurs around the LSPR peak (corresponding to a spectral red-shift of the peak, $\Delta\lambda_{peak}$) induced by a local permittivity change due to CO_2 adsorption.[12,14,22] Interestingly, similar changes occur in the extinction signal at the PIM-1 absorption band, ΔExt_{PIM}. To exclude any relation to a spectral overlap with the LSPR, a sample without plasmonic nanoparticles was also studied. It exhibits the same changes and corroborates an intrinsic optical response of the PIM-1 on CO_2 adsorption (see section S4 in the Supporting Information).

When measured as a function of time, the $\Delta\lambda_{peak}$ signal has a higher signal-to-noise ratio (SNR) than the ΔExt_{PIM} signal with respect to changes in the CO_2 pressure. The orange line in Figure 2c represents the ΔExt_{PIM} signal at 450 nm for a pressure change from 0 to 1 atm CO_2 and has a SNR of ∼26. It is improved to ∼71 by reading off its mean value in the range of 445−455 nm (red line). Notably, it is still significantly smaller than the SNR of 228 of the plasmonic readout signal $\Delta\lambda_{peak}$ shown in Figure 2d.

As shown in Figure 3a,b, the ΔExt_{PIM} and $\Delta\lambda_{peak}$ readouts during the CO_2 exposure of the PIM-1 film directly indicate variations in the amount of CO_2 adsorbed in the polymer with respect to partial pressures (ranging from 25−100% of 1 atm in 25% steps) and temperatures (298−358 K in 10 K steps). Specifically, we notice the direct correlation between the CO_2 concentration and temperature, and the magnitude of ΔExt_{PIM} and $\Delta\lambda_{peak}$, which is in line with the expected pressure and temperature dependence of the amount of adsorbed CO_2 in the polymer.[23]

The correlation between the ΔExt_{PIM} and $\Delta\lambda_{peak}$ signals is quantified by plotting the equilibrium $\Delta\lambda_{peak}$ values for each pressure and temperature condition as a function of the corresponding ΔExt_{PIM} value, as displayed in Figure 3c. Their linear relation almost perfectly converges toward the origin and corroborates that *identical* information is obtained from both readouts. This scaling is quite remarkable as the two readouts are mechanistically very different. For example, the ΔExt_{PIM} is an integration throughout the whole PIM-1 film, i.e., the signal is the result of the sum of all CO_2 molecules adsorbed in the sample. In contrast, plasmonic sensing only detects CO_2 adsorbed within the PIM-1 in a vicinity of a few tens of

DOI: 10.1021/acs.analchem.5b03108
Anal. Chem. 2015, 87, 10161−10165

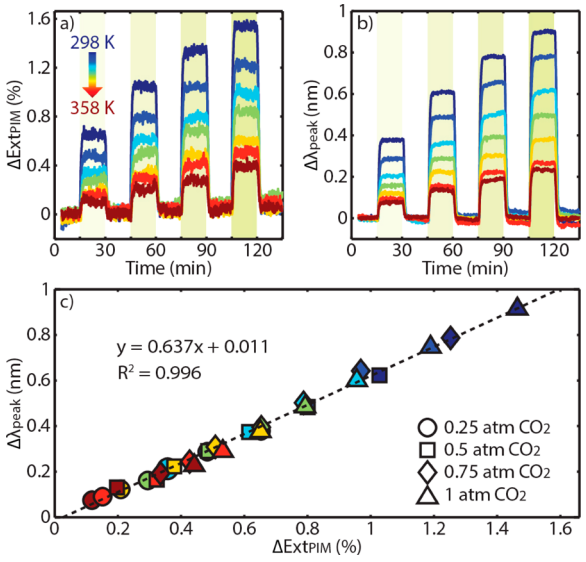

Figure 3. Time resolved (a) ΔExt_{PIM} and b) $\Delta\lambda_{peak}$ signals upon CO_2 sorption cycles for different CO_2 partial pressures, carried out at different temperatures (298−358 K, 10 K steps). (c) Direct correlation between the ΔExt_{PIM} and $\Delta\lambda_{peak}$ derived from the equilibrium signals obtained at all investigated temperatures (color code) and CO_2 pressures (symbols). The dashed line denotes a linear regression with an R^2 value of 0.996.

nanometers around the metal nanostructures, i.e., within the so-called sensing volume.[24] The perfect proportionality between the two readouts thus implies that the CO_2 adsorption is taking place homogeneously throughout the sample. At the same time, it also shows that the combination of these two readouts provides a means to identify possible heterogeneity in CO_2 adsorption properties throughout a material, since the plasmonic sensor only probes the internal interface.[24]

Using the temperature and pressure dependent data obtained above, we can now construct CO_2 adsorption isotherms from the ΔExt_{PIM} and $\Delta\lambda_{peak}$ responses, as shown in Figure 4. The

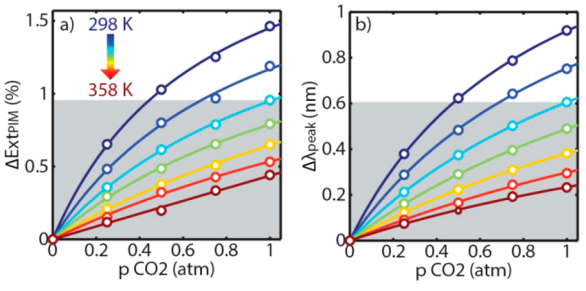

Figure 4. Optical CO_2 adsorption isotherms constructed from (a) ΔExt_{PIM} and (b) $\Delta\lambda_{peak}$ at different temperatures (298−358 K, 10 K steps). The solid lines correspond to a first order Langmuir adsorption regression analysis. The gray areas denote the regimes used for construction of isosteres and Clausius−Clapeyron analysis of the loading dependent isosteric heat of adsorption.

isotherms exhibit the expected dependencies on CO_2 partial pressure and temperature. Moreover, they are also in excellent agreement with first order Langmuir adsorption (solid lines, all regression parameters are available in the Supporting Information), as expected for CO_2 adsorption on glassy polymers.[23] Thus, our isotherms display perfect resemblance with conventionally measured pressure−composition ($p-C$) isotherms reported for the same system.[25,26] Therefore, the loading dependent Q_{st} of CO_2 is extracted by means of a Clausius−Clapeyron analysis, as shown in the isosteres of Figure 5a, which are constructed from the $p-T$ combinations in

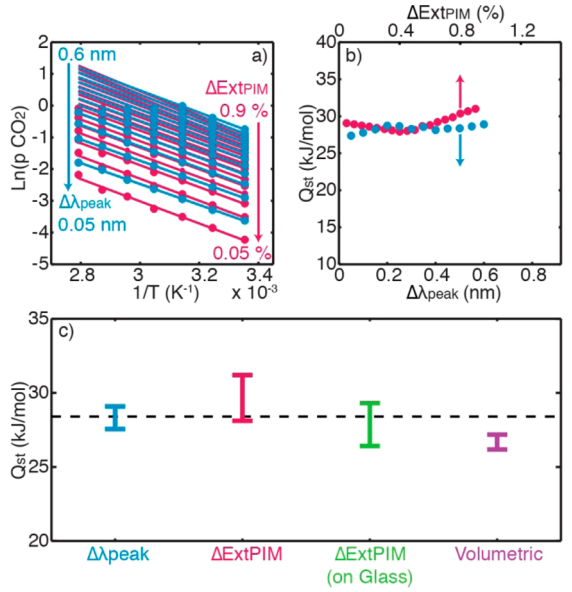

Figure 5. (a) Isosteres for Clausius−Clapeyron analysis from ΔExt_{PIM} (red) and $\Delta\lambda_{peak}$ (blue) readouts at constant optical signal values, i.e., CO_2 coverage. (b) The isosteric heats of adsorption, Q_{st}, obtained from the isosteres. Both analyses yield a very similar range of values between 27 and 31 kJ/mol. (c) Comparison of the loading dependent range of Q_{st} values. Data obtained from the ΔExt_{PIM}, the $\Delta\lambda_{peak}$ readouts of the INPS sensor sample, optical ΔExt_{PIM} measurement on a PIM-1 thin film directly on glass (i.e., without plasmonic nanoparticles) (green), and from conventional volumetric analysis of a PIM-1 sample synthesized in the same batch (purple). Note the good agreement between the different samples and detection modes as well as with the reported value from the literature, 28.4 kJ/mol (dashed line).[26]

Figure 4 at constant CO_2 coverage (corresponding to constant optical signal value).[27] An alternative analysis based on the Langmuir model is shown in the Supporting Information.

The loading dependent Q_{st} values are plotted in Figure 5b as a function of the optical signals ΔExt_{PIM} and $\Delta\lambda_{peak}$, which are proportional to the adsorptive loading of CO_2. Both optical readouts result in loading dependent Q_{st}, spanning a range of 27−31 kJ/mol. Moreover, as expected, we find that Q_{st} is independent of the PIM-1 film thickness as shown in Figure S15 in the Supporting Information.

As the last step of our analysis, the Q_{st} values are put in perspective. Figure 5c quantitatively compares the obtained numbers with additional results from an optical measurement with PIM-1 directly on glass (i.e., no plasmonic nanoparticles) as well as a sample characterized using conventional volumetric analysis (see the Supporting Information). Clearly, our optically derived results are in very good agreement with each other as well as with the 28.4 kJ/mol (dashed line) reported in the literature.[26] The agreement with our Q_{st} derived from the volumetrically determined isotherms (26−27 kJ/mol) is also very reasonable.

In summary, we demonstrate two simple yet very effective optical *in situ* characterization methods to reveal the adsorption energetics of CO_2 for porous materials targeting CCS or other

DOI: 10.1021/acs.analchem.5b03108
Anal. Chem. 2015, 87, 10161−10165

CO_2/gas separation processes. They are based on UV−vis spectroscopy or nanoplasmonic sensing. Specifically, we observe CO_2 adsorption isotherms by either monitoring the direct optical extinction change of the UV−vis spectroscopic band of the PIM-1 itself or by tracking the spectral position of the plasmon resonance in gold sensor nanoparticles adjacent to the PIM-1. The optical signals from both methods are directly proportional with each other as well as with the CO_2 coverage in the adsorbent, as corroborated by the excellent agreement with first order Langmuir adsorption. Thus, from our optical isotherms we can derive the Q_{st} of CO_2 based on a Clausius−Clapeyron analysis (or the Langmuir adsorption model as shown in the Supporting Information). The average value of Q_{st} is ∼29 kJ/mol and thus in good agreement with the literature as well as with our own control experiment using a volumetric technique.

These results have several key implications. The first one is that, as opposed to the traditionally used gravimetric or volumetric characterization, here we *directly* measure the adsorbed CO_2 on the adsorbent. This eliminates the need to calibrate the sample thickness, mass, and/or volume. The second one is that, for CO_2 adsorbents with absorption bands in the UV−vis range, simple UV−vis spectroscopy can be used for adsorption characterization. This fast and low cost method could be particularly well suited for rapid materials screening and complement methods based on infrared spectroscopy. For transparent materials, the plasmonic sensing approach is attractive, because it provides the necessary optical contrast. Moreover, as we have shown, it generally yields significantly higher SNR than the simple UV−vis method and thus allows experimental investigations with higher resolution. Finally, the two readouts *in combination*, if spectrally detuned as demonstrated here, can provide an efficient means to characterize the homogeneity of the adsorbent as well as diffusion related effects because they are based on two mechanistically different readout principles.[24] The extinction change upon adsorption of CO_2 in the spectral band region of the PIM-1 corresponds to a signal proportional to the *integrated* CO_2 adsorption. In contrast, the plasmonic sensors located at the internal interface between the adsorbent layer and support is only a *local* probe with a sensing volume that extends a few tens of nanometers from the plasmonic sensor particle surface. In view of the above and the generic nature of our approach, we predict that this method could be extended to other adsorbate−adsorbent systems (e.g., MOFs[14] and SURMOFs[28] grown on surfaces) to quantify their interactions, independent of whether the adsorbent exhibits its own optical absorption band(s) or is completely transparent. However, our approach is ideally suited for polymeric or molecular based porous films that can be rapidly deposited on the sensors.

■ ASSOCIATED CONTENT

Supporting Information

The Supporting Information is available free of charge on the ACS Publications website at DOI: 10.1021/acs.analchem.5b03108.

Experimental details, PIM-1 molecular characterizations, results and analysis for the PIM-1 directly on glass, volumetric adsorption measurement, Langmuir adsorption model, Q_{st} derived from Langmuir model and thickness dependence of optically derived Q_{st} (PDF)

■ AUTHOR INFORMATION

Corresponding Author

*E-mail: clangham@chalmers.se.

Author Contributions

The manuscript was written through contributions of all authors. All authors have approved the final version of the manuscript.

Notes

The authors declare no competing financial interest.

■ ACKNOWLEDGMENTS

We acknowledge financial support from the Swedish Research Council (VR), the Swedish Foundation for Strategic Research Framework Program RMA11-0037, the Chalmers Area of Advance for Nanoscience and Nanotechnology, the Knut and Alice Wallenberg Stiftelse for their support of the infrastructure in the MC2 nanofabrication laboratory at Chalmers, and the Swedish Research Council for their support of the μ-fab cleanroom infrastructure in Sweden. N.H. thanks the Swedish Energy Agency and VR and VINNOVA for support.

■ REFERENCES

(1) Lacis, A. A.; Schmidt, G. A.; Rind, D.; Ruedy, R. A. *Science* **2010**, *330* (6002), 356−359.

(2) Sumida, K.; Rogow, D. L.; Mason, J. A.; McDonald, T. M.; Bloch, E. D.; Herm, Z. R.; Bae, T.-H.; Long, J. R. *Chem. Rev.* **2012**, *112* (2), 724−781.

(3) D'Alessandro, D. M.; Smit, B.; Long, J. R. *Angew. Chem., Int. Ed.* **2010**, *49* (35), 6058−6082.

(4) Choi, S.; Drese, J. H.; Jones, C. W. *ChemSusChem* **2009**, *2* (9), 796−854.

(5) Nugent, P.; Belmabkhout, Y.; Burd, S. D.; Cairns, A. J.; Luebke, R.; Forrest, K.; Pham, T.; Ma, S.; Space, B.; Wojtas, L.; Eddaoudi, M.; Zaworotko, M. J. *Nature* **2013**, *495* (7439), 80−84.

(6) Lin, L.-C.; Berger, A. H.; Martin, R. L.; Kim, J.; Swisher, J. A.; Jariwala, K.; Rycroft, C. H.; Bhown, A. S.; Deem, M. W.; Haranczyk, M.; Smit, B. *Nat. Mater.* **2012**, *11* (7), 633−641.

(7) Bae, Y.-S.; Snurr, R. Q. *Angew. Chem., Int. Ed.* **2011**, *50* (49), 11586−11596.

(8) Keller, J. U.; Robens, E.; du Fresne von Hohenesche, C. *Characterization of Porous Solids VI, Proceedings of the 6th International Symposium on the Characterization of Porous Solids (COPS-VI)*; Studies in Surface Science and Catalysis, Vol. *144*; Elsevier: Amsterdam, The Netherlands, 2002.

(9) Keller, J. U.; Rave, H.; Staudt, R. *Macromol. Chem. Phys.* **1999**, *200* (10), 2269−2275.

(10) Langhammer, C.; Larsson, E. M.; Kasemo, B.; Zorić, I. *Nano Lett.* **2010**, *10* (9), 3529−3538.

(11) Bohren, C. F.; Huffman, D. R. *Absorption and Scattering of Light by Small Particles*; Wiley-VCH: New York, 2007.

(12) Tittl, A.; Giessen, H.; Liu, N. *Nanophotonics* **2014**, *3* (3), 157−180.

(13) Mayer, K. M.; Hafner, J. H. *Chem. Rev.* **2011**, *111* (6), 3828−3857.

(14) Kreno, L. E.; Hupp, J. T.; Van Duyne, R. P. *Anal. Chem.* **2010**, *82* (19), 8042−8046.

(15) Dahlin, A. B.; Tegenfeldt, J. O.; Höök, F. *Anal. Chem.* **2006**, *78* (13), 4416−4423.

(16) Budd, P. M.; Elabas, E. S.; Ghanem, B. S.; Makhseed, S.; McKeown, N. B.; Msayib, K. J.; Tattershall, C. E.; Wang, D. *Adv. Mater.* **2004**, *16* (5), 456−459.

(17) Budd, P. M.; Ghanem, B. S.; Makhseed, S.; McKeown, N. B.; Msayib, K. J.; Tattershall, C. E. *Chem. Commun. (Cambridge, U. K.)* **2004**, *2*, 230−231.

(18) Budd, P. M.; McKeown, N. B.; Fritsch, D. *Macromol. Symp.* **2006**, *245*−*246* (1), 403−405.

DOI: 10.1021/acs.analchem.5b03108
Anal. Chem. 2015, 87, 10161−10165

(19) Du, N.; Park, H. B.; Robertson, G. P.; Dal-Cin, M. M.; Visser, T.; Scoles, L.; Guiver, M. D. *Nat. Mater.* **2011**, *10* (5), 372−375.
(20) Robeson, L. M. *J. Membr. Sci.* **2008**, *320* (1−2), 390−400.
(21) Gusak, V.; Heiniger, L.-P.; Graetzel, M.; Langhammer, C.; Kasemo, B. *Nano Lett.* **2012**, *12* (5), 2397−2403.
(22) Wadell, C.; Nugroho, F. A. A.; Lidström, E.; Iandolo, B.; Wagner, J. B.; Langhammer, C. *Nano Lett.* **2015**, *15* (5), 3563−3570.
(23) Paul, D. R. *Ber. Bunsenges. Phys. Chem.* **1979**, *83* (4), 294−302.
(24) Gusak, V.; Heiniger, L.-P.; Zhdanov, V. P.; Grätzel, M.; Kasemo, B.; Langhammer, C. *Energy Environ. Sci.* **2013**, *6* (12), 3627−3636.
(25) Li, P.; Chung, T. S.; Paul, D. R. *J. Membr. Sci.* **2014**, *450*, 380−388.
(26) Patel, H. A.; Yavuz, C. T. *Chem. Commun. (Cambridge, U. K.)* **2012**, *48* (80), 9989−9991.
(27) Sircar, S. *J. Chem. Soc., Faraday Trans. 1* **1985**, *81* (7), 1527−1540.
(28) Heinke, L.; Tu, M.; Wannapaiboon, S.; Fischer, R. A.; Wöll, C. *Microporous Mesoporous Mater.* **2015**, *216*, 200−215.

DOI: 10.1021/acs.analchem.5b03108
Anal. Chem. 2015, 87, 10161−10165